Published in final edited form as:

Nature. 2018 September ; 561(7724): 542–546. doi:10.1038/s41586-018-0527-y.

Sensation Movement and Learning in the Absence of Barrel Cortex

Y. Kate Hong, **Clay O. Lacefield**, **Chris C. Rodgers**, and **Randy M. Bruno***

Department of Neuroscience, Mortimer Zuckerman Mind Brain Behavior Instituteand Kavli Institute for Brain Science, Columbia University, New York, NY 10027, USA

Abstract

For many of our senses, the role of the cerebral cortex in detecting stimuli is controversial[1–17]. Here, we examine the effects of both acute and chronic inactivation of primary somatosensory cortex (S1) in mice trained to move their large facial whiskers to detect an object via touch and respond with a lever to obtain a water reward. Using transgenic animals, we expressed inhibitory opsins in excitatory cortical neurons. Transient optogenetic inactivation of S1, as well as permanent lesions, initially produced both movement and sensory deficits that impaired detection behavior, demonstrating the inextricable link between sensory and motor systems during active sensing. Surprisingly, lesioned mice rapidly recovered full behavioral capabilities by the subsequent session. Recovery was experience-dependent, and early re-exposure to the task after lesion facilitated recovery. Furthermore, primary sensory cortex ablation prior to learning did not affect task acquisition. This combined optogenetic and lesion approach suggests that manipulations of sensory cortex may be only temporarily disruptive to other brain structures, which are themselves capable of coordinating multiple, arbitrary movements with sensation. Thus, the somatosensory cortex may be dispensable for active detection of objects in the environment.

Sensory detection tasks have become a staple for probing cortical circuitry during behavior, but the role of primary sensory cortex in such visual[1–3], auditory[4–6], gustatory[7,8], and somatosensory behaviors[9–17] remains unclear. The causal role of a brain structure is typically assessed by inactivation or ablation. Ablations may underestimate behavioral deficits, due to long recovery periods used (>1 week) during which compensatory relearning or rewiring can occur. Transient optogenetic or pharmacological manipulations often yield stronger deficits and are currently preferred, being thought to reveal an area's normal function prior to compensation. However, the sudden loss of a silenced area may disrupt downstream areas vital to behavior, a phenomenon known as *diaschisis*. Recent studies

*CORRESPONDENCE Randy M. Bruno, 3227 Broadway, Room L7-008, Mail Code 9871, New York, NY 10027, randybruno@columbia.edu.

Author Contributions

YKH and RMB conceived the experiments, analyzed data, and wrote the manuscript. YKH performed the experiments. COL and YKH developed the behavioral assay. CCR assembled videography setup, CCR and YKH performed array recordings, and CCR analyzed array data.</author_notes>

The authors declare no competing financial interests.

underscored how off-target effects of transient inactivation can lead to false conclusions[18]. To address these disparate outcomes, we compare transient and chronic manipulations of the barrel cortex subdivision of S1 during a simple detection behavior.

Water-restricted mice were trained in the dark to perform a go/nogo sensory detection task with their C2 whisker (Fig. 1a). Animals self-initiated trials by holding down a lever. On "go" trials, a pole moved within reach of the whisker when protracted. Mice released the lever to indicate pole detection to obtain a water reward (hit). On "nogo" trials, the pole moved away from the mouse. Incorrect responses to nogo trials (false alarms) were punished with a timeout. Misses and correct rejects were neither rewarded nor punished.

Conventionally, cortex is optogenetically silenced by activating inhibitory cells with channelrhodopsin (ChR), but this may inadvertently stimulate long-range inhibitory connections. We therefore developed an approach to directly silence excitatory cells by stably expressing halorhodopsin (Halo) in cortical excitatory neurons. Emx1-Halo mice enable targeted, stable expression of reporter genes in excitatory cortical neurons while excluding subcortical structures (Fig. 1b). Optogenetic silencing during behavior was highly efficacious, blocking 95±4% (mean±SEM) spikes in putative excitatory cells (Fig. 1c-e, Extended Data Fig. 1j-k), including during whisker contacts, which normally strongly activate barrel cortex (Fig. 1f). Optogenetics efficiently silenced spontaneous and sensory-evoked activity in neurons across all cortical layers within a 1-mm radius, encompassing nearly all the barrel columns representing the large facial whiskers (Extended Data Fig. 1a-i).

Inactivation of barrel cortex significantly reduced overall performance (n=10 mice; Fig. 1g, Extended Data Fig. 2a) but remained above 50% chance ($p=2.3\times10^{-4}$, t-test). Despite fewer responses to both go and nogo trials (Fig. 1h,i), response time was unaffected by the laser (Fig. 1j), demonstrating the animals' continued ability to maneuver the lever. Control mice lacking Cre were behaviorally unaffected by the laser (n=7 stop-Halo mice; Fig. 1g-j). Conventional photoinhibition by activating inhibitory cells (n=5 PV-ChR mice*)* yielded similar results to Emx1-Halo (Extended Data Fig. 2a). Thus, transiently silencing barrel cortex significantly impaired detection behavior.

Touch is an active process, whereby subjects adjust their movements in response to contacting objects in their environment[19–21]. Even small changes in whisking could alter perception[19]. While activation of barrel cortex can trigger whisker movements[16,22], the effects of inactivation are less understood[12,23]. We tracked whisking with high-speed videography (Fig. 2a,b). During nogo trials, in which no contacts are possible, barrel cortex inactivation slightly but significantly decreased protraction velocity, whisker angle, and peak amplitude (Fig. 2c-f). Similarly, during go trials when the pole is present, inactivation of barrel cortex decreased peak protraction velocity (Fig. 2g). No significant changes in whisking setpoint or frequency were detected. We additionally assessed change in whisker curvature, a proxy for contact force[24] (Extended Data Fig.3). Small changes in whisker movement had a large effect on whisker contacts, resulting in less force (Fig. 2h) and more trials without contacts (Fig. 2i). Thus, silencing of sensory cortex reduced the vigor of whisker movement.

We asked whether behavioral impairment was simply due to altered whisking or whether there was an accompanying sensory deficit: for any given stimulus strength, does transient inactivation decrease the probability of response? Cortical silencing significantly increased detection threshold (0.5 response probability) for curvature (Fig. 2j,k) and number of contacts (Fig. 2m,n), but not sensitivity (Fig. 2l,o). We observed similar motor and sensory deficits in PV-ChR mice (Extended Data Fig. 2b,c). Thus, transient optogenetic manipulations impair behavior by both increasing sensory threshold and decreasing whisker movement.

Increased sensory threshold is distinct from an absolute inability to detect stimuli. The observed threshold shift could reflect incomplete inactivation, since a few renegade spikes may suffice for detection[25]. However, residual spiking during optogenetic silencing did not correlate with behavioral outcome (Extended Data Fig. 1l,m). To ensure complete inactivation, we removed contralateral barrel cortex by aspiration (n=11) (Fig. 3a,b; Extended Data Fig. 4). Consistent with optogenetic results, behavior was impaired 1 day after lesioning contralateral barrel cortex (Fig. 3c, red), but not in sham-operated controls (n=4; black) or when ipsilateral barrel cortex was lesioned (n=4; blue). Again, impairment was only partial, and behavior remained significantly above chance levels ($p<10^{-6}$, t-test).

Surprisingly, by the second post-lesion session, behavior fully recovered to pre-lesion levels (Fig. 3c). Mice recovered whether lesions encompassed only barrel cortex or additionally included secondary somatosensory cortex (Extended Data Fig. 4). There was no evidence of gradual relearning within sessions; rather, performance abruptly recovered between the 1st and 2nd post-lesion sessions (Fig. 3d), suggesting that recovery was unlikely to result from previously uninvolved circuits learning the task anew. Furthermore, subsequently lesioning ipsilateral barrel cortex did not perturb performance, as these bilaterally lesioned animals performed similar to sham and ipsi-only lesioned mice (Extended Data Fig. 5). Interestingly, additional damage to dorsolateral striatum prevented behavioral recovery (Fig.3c, n=8, orange; Extended Data Fig. 6), suggesting an important role of this area in detection behavior.

Consistent with optogenetic results, whisker movement and contacts decreased on the first post-lesion session (Fig. 3e,f, “pre” vs. “1”). However, whisking kinematics for the recovered, second session never exceeded pre-lesion levels (Fig.3e,f; “pre” versus “2”), indicating that mice did not compensate for impaired sensation with greater contact force or frequency. Similarly, sensory thresholds pre-lesion and on the second post-lesion session did not significantly differ in contact force or number (Fig. 3h,i). Thus, after only a temporary impairment, both motor and sensory abilities returned to pre-lesion levels along with behavioral performance.

Recent studies suggest that homeostasis may spontaneously restore activity in connected structures within a similar time frame of 24–48 hours[18,26]. In order to test whether behavioral recovery was spontaneous or required re-exposure to the task, we gave another group of animals three days between lesion and retesting (n=8). This group showed similar impairment on the first post-lesion session but also recovered (Fig. 3j), albeit more gradually, indicating that task re-exposure, rather than simply the passage of time, triggers

recovery. Removing the C2 whisker reduced performance of both 1- and 3-day-rest groups to chance, confirming that lesions did not induce mice to switch from whisker-mediated touch to other sensory modalities (Fig. 3g,k).

Thus, three different manipulations of barrel cortex—Emx1-Halo, PV-ChR and lesions—are transiently disruptive to executing active detection behavior. Recent studies have demonstrated that motor cortex may not be required for execution of skilled movements, but is required for motor learning[27]. To determine whether sensory cortex is required for learning the detection task, we lesioned contralateral S1 of naïve mice. Subjects were habituated and trained on lever maneuvering. Learning rate was assessed starting with the introduction to the pole (Fig. 4a, learning assessment, red). Initially sessions consisted of 90% go trials until animal weight stabilized (3.6±1.5 sessions), after which mice still performed at chance (Extended Data Fig. 7a-c). Lesioned and unlesioned animals learned at similar rates (Fig. 4b,c). Non-learners were equally present in both groups (Fig. 4d, 6/17 unlesioned, 5/14 lesioned, p=1, Fisher's exact test), and failure to learn was uncorrelated with lesion size (Fig. 4e). In fact, among learners, animals with larger lesions learned faster than those with smaller lesions (Fig. 4e, linear regression, p=0.02). Again, performance remained whisker-dependent (Fig. 4f,g). Thus, barrel cortex is nonessential for learning the detection behavior.

Task acquisition involves motor (lever press/lift), perceptual (pole detection), and contingency learning (lever→reward, contact→lever→reward). Importantly, mice acquired the task whether lesioned prior to handling and lever training (Fig.4a, open triangle, n=4) or just prior to introduction of the pole (closed triangle, n=5). Mice spent similar amounts of time in pretraining whether lesioned prior to pretraining or unlesioned (p=0.13). Thus, barrel cortex appears not required for motor, perceptual, and contingency learning of this task.

Our results demonstrate the potential for pathways other than sensory cortex to direct learned behaviors requiring arbitrary coordination of multiple movements (lever press, whisking, licking) around a sensory event. This raises concerns with interpretation of cortical physiology studies utilizing detection behaviors. It underscores the need to identify the behavioral conditions for which barrel cortex is indispensable, which might involve more complex discrimination, egocentric or allocentric context[10,28], or working memory[29].

In conclusion, impairment after transient inactivation does not absolutely indicate necessity. What then is the functional relevance of barrel cortex to active detection? One possibility is that the barrel cortex and other structures are redundant for active detection[30]. Multiple subcortical structures are recipients of barrel cortex input and, via other routes, whisker-related sensory signals. The trigeminal brainstem complex projects directly to superior colliculus and cerebellum, and indirectly to dorsolateral striatum via secondary somatosensory thalamus[30–32]. Indeed, damage to striatum prevented recovery. Further studies are needed to assess the roles of other subcortical areas.

A second possibility is that manipulating any cortical area may temporarily disrupt connected structures primarily involved in the task. In this scenario, the sudden loss of barrel cortex activity, rather than the sensory information it conveys, can be disruptive. The

incomplete behavioral impairments we observed as well as sudden recovery after lesion raise the possibility of a disruptive effect, rather than redundancy. Subcortical systems are major targets of deep layer cortical pyramidal cells, which have high baseline firing rates, and removing their tonic activity may disrupt responses of corticofugal targets to sensory inputs. In the birdsong motor system, lesions transiently disrupted activity in downstream areas and the production of song, both of which recovered overnight[18]. It was unclear if recovery was spontaneous or required some attempts, even if unsuccessful, at singing. A major advantage of our study is that we could control the time of re-exposure to the task after lesioning. Early task-specific experience accelerated recovery, which may have important implications for early rehabilitation after stroke or head trauma. Whether recovery is always experience-dependent or whether sensory and motor systems differ are intriguing candidates for further study.

METHODS

Transgenic Animals.

All animal procedures complied with the NIH Guide for the Care and Use of Laboratory Animals and were approved by the Institutional Animal Care and Use Committee at Columbia University. Emx1-Halo mice (n = 10) were generated by crossing Emx1-IRES-Cre[33] knock-in mice (Jackson Laboratories, stock #005628) to Rosa-lox-stop-lox (RSL)-eNpHR3.0/eYFP mice (“stop-Halo” Ai39, JAX, stock# 006364), which express halorhodopsin after excision of a stop cassette by Cre recombinase. Cre expression was assessed by crossing Emx1-Cre mice to RSL-H2B-GFP mice (provided by J. Huang). Negative control animals were Cre-negative and could not express the halorhodopsin transgene (n = 7 stop-Halo mice). PV-ChR mice (n=5) were generated by crossing Parvalbumin-Cre mice[34] to RSL-Channelrhodopsin2/eYFP (Ai32, Jackson Laboratories, stock# 024109). For visualizing barrel neurons in S1, Nr5a1-Cre mice (JAX, stock# 006364) were crossed to RSL-Halo-eYFP (Nr5a1-eYFP). All mouse lines were maintained on a C57BL/6 background. Optogenetic experiments utilized mice that were heterozygous for the desired transgene.

Behavioral setup.

The behavioral setup was controlled by a microcontroller (Arduino), and data collected using custom written routines. Subjects self-initiated trials by holding down a lever with their left forepaw for at least 100 msec. A pole (~2.15-mm diameter wooden applicator stick) started from a position 3–4 cm below the animal. After trial initiation, a stepper motor (Pololu Robotics and Electronics) rotated the pole to just in front of the whiskers (go trials) or away from the whisker field entirely (nogo trials). Rotation in either direction ensured that the sound and vibration generated by the motor was similar between trial types. The sound of the motor also served as a trial onset and offset cue. For go trials, the pole was positioned 9–11 mm laterally and roughly aligned to the tip of the nose in the anterior-posterior dimension, such that animals were required to actively whisk forward to make contact. If the lever was lifted within the response window of 1.2 seconds during go trials (hit), the response was rewarded with a drop of water and a reward tone. False alarm responses during nogo trials were punished with a timeout period of 3–8 seconds accompanied by white noise

sound, during which the mouse could not initiate a new trial. There was no reward for a correct reject and no punishment for a miss. The response latency was defined as the time from when the pole was first within reach of the animal's whisker (typically 480ms from trial onset, identified from high-speed video for each session analyzed) to the animal's lever lift response.

Intrinsic signal optical imaging to locate C2 barrel.

Animals were anesthetized with isoflurane, and the skull over the left barrel cortex (centered ~1.5 mm posterior of bregma and 3.5mm lateral of the midline) was thinned and sealed with Vetbond (3M) over a 4–5 mm area, or a glass window (3-mm coverslip, Warner Instruments) was implanted. Images were acquired with a CCD camera (Q-Imaging, Retiga 2000R) mounted on a stereomicroscope and software custom-written in LabVIEW. The vasculature on the brain surface was imaged with 510/40 band-pass filtered illumination (Chroma, D510/40), and functional imaging done with illumination with a 590-nm long-pass filter (Thorlabs, OG590). The C2 whisker was stimulated with 8 pulses of 4 directions at 5Hz with a multi-directional piezo stimulator. The location of the maximum reflectance change was mapped relative to the surface vasculature. 2–3 surrounding whiskers were also imaged to confirm proper identification of the C2 barrel location.

Animal training.

Test of task performance.—Adult mice (P116 ± 60 days, mean and standard deviation, 34% male) were implanted with a custom-designed 22-guage stainless steel laser-cut (Laser Alliance) headplate with dental acrylic. After ~1 week of recovery, subjects in optogenetics experiments were water-restricted and habituated through a series of pre-training stages: (1) freely-moving animals were habituated to the behavioral apparatus, where water reward was given for holding down a lever (2–3 days). (2) Mice were head-fixed and continued lever training (2–3 days): water was awarded for holding down lever for 500ms to initiate trial (2–4 days), followed by releasing the lever for >100ms (2–4 days). (4) For all subsequent stages, animals were trained in a dark chamber where no visual cues could be used. Animals were trained with 90% go trials with a pole, and received water for responding by lifting a lever on go trials, or a 3–5 second timeout if response was on a nogo trial (2–8 days). We found that adding this gradual training stage with 90% go-trials facilitated learning. Once animal weight stabilized at this stage, mice were trained at 60% go trials until learning criterion (defined as >74% correct performance for 2 consecutive days) was reached.

Once subjects learned the detection task with all whiskers intact, the location of the C2 barrel was functionally mapped using intrinsic signal optical imaging. All whiskers except C2 on the animal's right side were trimmed. Animals were retrained with a single C2 whisker until >74% performance was reached with 50% go trials. In most cases, behavioral performance dropped after the initial whisker trimming but recovered over 1–7 days. Trimming was maintained twice a week. Lesions or sham operations were made after animals' performance stabilized above the performance criterion. Any animals could still perform well (>60% correct) in the absence of all whiskers and were excluded from analysis.

Test of task learning.—For learning experiments, mice were trained as above but with more standardized training periods. Mice recovered from surgery and were habituated to handling by the trainer for 1–2 days. Mice were water-restricted and habituated through a series of pre-training stages. Progression through each step depended on the individual mouse's weight stabilization (indication of health), or whether rest days (weekends) interrupted training, rather than an explicit behavioral criterion. (1) Freely-moving animals were habituated in the light to the behavioral apparatus, where water reward was given for holding down a lever (1–2 days). (2) Mice were head-fixed and continued to hold down the lever to drink (4±2 days, mean and standard deviation). (3) Mice were rewarded for holding down the lever and subsequently lifting for >100 ms (4±2 days). All whiskers excluding C2 were trimmed twice a week for the remainder of the learning experiment. We quantified learning time for the following stages: mice were first introduced to the pole with 90% go trials (~4 days, See Extended Data Fig.7). This stage and successive ones were performed in a light tight box where no visual cues could be used. Mice were given <48 sessions to reach learning criterion of 74% correct for 2 consecutive sessions. To factor in the different number of go and nogo trials, we calculated % correct performance as 100 * (N_{hit}/N_{go} + N_{CR}/N_{nogo})/2 where the N's are the numbers of hit, go, correct reject, and nogo trials.

A total of 29 animals were lesioned prior to learning. Of these, several animals were excluded from analysis, including: 6 animals that performed >60% correct after full whisker trimming; 3 animals that were found to have lesions that did not include the C2 barrel; and 6 animals that had lesions that extended below the cortex, including white matter and striatum.

Quantification of whisker movements and contacts.

Whisking was monitored with a high-speed camera (Photonfocus AG, MV1-D1312–100-G2) at 250 fps and 640×480 pixels/frame under infrared illumination. Whiskers were automatically traced offline and whisker position (angle) and curvature were obtained using Whisk[35,36]. Trials in which tracing failed >10% of frames were omitted from analysis.

For each session, animals were given a 5-min warm-up before analysis began, except for quantification of within-session performance (Fig. 3d) where the entire trial was included for analysis. Whisking analysis was restricted to a 200-ms window starting from the first frame in which whisker contact with the pole was possible. This window was chosen to best isolate the whisking associated with the sampling of the object and before the response, after which, whisking tended to increase in association with licking for water reward (Fig. 2g). For whisking amplitude and phase, the azimuthal whisking angle was band-pass filtered (four-pole Butterworth, 4–50 Hz) followed by a Hilbert transform[37,38]. Instantaneous frequency was calculated from the phase. The setpoint was measured as the midpoint between the whisking envelope defined by the maximum and minimum whisker angles for each whisk cycle.

Whisker contacts were defined using whisker angle and curvature parameters for each session. We first determined the range of angle-curvature values during free whisking in air (nogo trials). The baseline curvature for each trial (mean change in curvature during 200-ms period before each trial onset) was subtracted to obtain the change in curvature (ΔK). Linear regression of the whisker angle and change in curvature was used to find the line of best fit

(Extended Data Fig. 3). Upper and lower contact thresholds were set by finding the offset of the lines that encompassed the angle-curvature parameter space for all nogo trials (1–5 standard deviations). Putative contacts were defined as points at which local maxima or minima of ΔK were above or below the defined contact thresholds.

Optogenetic modulation of cortical activity.

For optogenetic experiments during detection behavior, the laser was on for 33–50% of trials, which were randomly interleaved with laser-off trials. For laser-on trials, an optical shutter opened at the onset of the trial, before movement of the pole. The pole moved within reach of the whisker field 200–400ms after the onset of the laser, ensuring photoinactivation before contacts were possible. The laser remained on until after the animal responded, or for the duration of the trial if no response was made, for a maximum of 1.5 seconds. Spiking activity during photoinhibition could be efficiently silenced for at least 2 seconds; all trials were 1.2–1.5 s in duration with a 1 second inter-trial-interval (Extended Data Fig. 1). Exposure to laser was limited to minimize photodamage to tissue. With the protocol described, no physiological or physical damage was detectable. A 593- or 594-nm laser (OEM or Coherent) was used with Emx1-Halo mice. For PV-ChR mice, an optical chopper (Thorlabs, MC2000B) modulated the 4 mW output of a 473-nm laser (OEM) to produce pulses at 40 Hz. Lasers were coupled to a 200-μm diameter, 0.39 NA optic fiber (Thorlabs) via a fiberport, and the diamond-knife cut fiber tip was placed above the optical window and positioned over C2 using the vasculature-referenced intrinsic signal map.

Electrophysiology.

Emx1-Halo animals (n=4) were habituated to head-fixation prior to recording. Juxtasomal recordings were made using pipettes filled with artificial cerebral spinal fluid and an Axoclamp 900A amplifier. Airpuff stimuli for each test condition were delivered by opening an air valve for 50 ms during trials ranging from 0.5 to 2 seconds, and an inter-trial interval of 1.5–3 sec for 30–50 trials. Laser-on trials were randomly interleaved for 50% of the trials. Glass pipettes were inserted perpendicular to the cortical surface (~30º from vertical), and the optic fiber was positioned vertically near the pipette entry point, above a thinned skull. For testing the effect of photoinhibition at various distances, the optic fiber was positioned 0.5, 1, 1.5, and 2 mm from the original recording site along a thinned and transparent skull (n = 21, 11, 10, 12, 16 respectively). Regular spiking (RS, putative excitatory) versus fast-spiking (FS, putative inhibitory) cells were categorized based on their spike waveforms as previously described[39]. Cortical depth was defined as the microdrive depth relative to the pial surface.

For recordings during the behavioral task, a linear silicon array (Cambridge NeuroTech H3), consisting of 64 sites spanning 1275 μm, was used. Each site was 11 × 15 μm and coated with PEDOT to obtain an impedance of 50–150 kΩ. Signals were bandpassed filtered 1–7500 Hz and sampled at 30 kHz (OpenEphys). Between sessions, the array was withdrawn and the craniotomy sealed with silicone. Spikes were clustered and inspected using Kilosort[40] and Phy[41].

Cortical lesions.

Mice were deeply anesthetized under isoflurane. A 1–4 mm craniotomy was made and the underlying cortical tissue was aspirated with a sterile blunt-tipped syringe needle connected to a vacuum. Lesions were made by aspirating all cortical layers to encompass, at a minimum, the C2 barrel and the immediately adjacent barrels, and at a maximum, the majority of S1 representing the large whiskers (macrovibrissae) and secondary somatosensory cortex (Extended Data Fig. 4, 5). Sham-operated mice were anesthetized under the same conditions, and the skull was thinned with a dental drill. Lesioned and sham-operated mice were allowed to recover for 1 or 3 days after surgery prior to testing. After behavioral testing was complete, animals were perfused and brains extracted for histological analysis. Brains were sectioned tangentially or coronally (100 μm) with a vibratome. Lesion diameter was quantified in ImageJ by outlining the lesioned area for each section, and quantifying the mean Feret diameter and averaging across all sections. Volume was measured by summing each section's lesion area multiplied by 100 (the section thickness).

In some cases, lesions extended beyond S1 and into subcortical tissue including the striatum. To objectively score striatal damage, the extent of cortical and subcortical damage was scored by raters experienced at looking at coronal sections of mouse brains and blind to the behavioral data (n=5).

Data analysis.

Analyses were done with custom-written scripts in MATLAB. For all figures, statistical significance is denoted as *: $p < 0.05$, **: $p< 0.01$, ***: $p<0.001$. No significant difference ($p>0.05$) unless otherwise indicated. Non-normally distributed data (D'Agostino-Pearson test) were quantified using medians and interquartile ranges, and normally distributed data with means and SEMs, using two-sided paired t-tests unless otherwise indicated. Based on the mean and standard deviation of normal performance levels of trained animals, power analysis indicated that detecting a drop in performance to chance levels with a significance criterion of 0.05 required a minimum sample size of 3, which we exceeded in all cases.

Code and data availability.

All computer code and data are available from the corresponding author upon reasonable request.

Extended Data

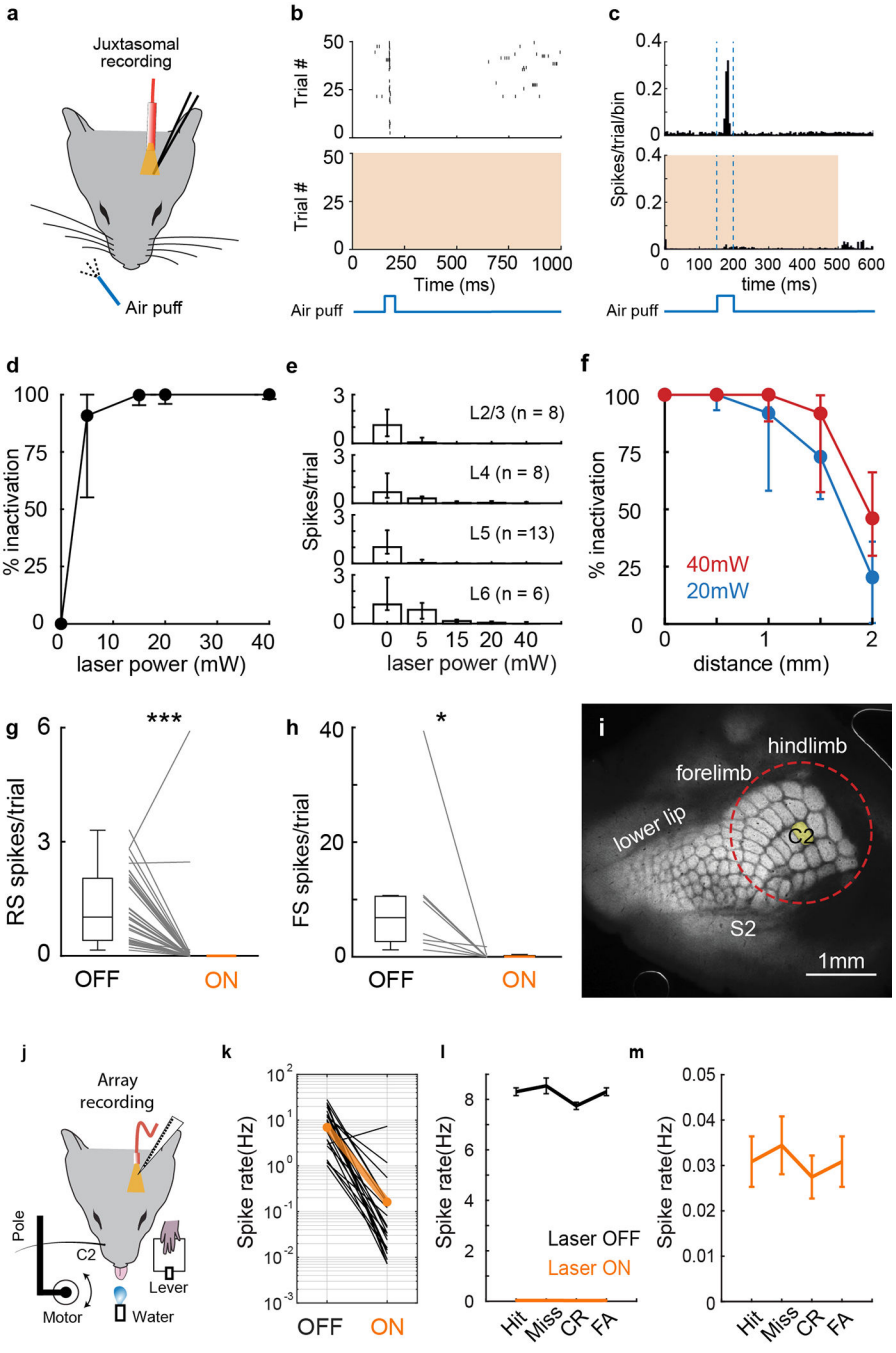

Extended Data Figure 1 |. Optogenetic photoinhibition of cortical neurons in Emx1-Halo is highly efficacious.

a, Juxtasomal recordings in awake, head-fixed mice were made below an optic fiber placed above a thinned, transparent skull. **b,** Raster plot for example neuron for randomly interleaved laser off (top) or on (bottom) trials, with air puff schematized below. **c,** Population peri-stimulus time histograms of 35 cell with regular-spiking (RS) waveforms (cortical depth: 280–1120 ¼m, n=4 mice) for laser-off and -on trials. Both spontaneous and

whisker stimulus-evoked spikes are silenced. Shaded area: laser on. **d,** Efficiency of RS cell inactivation by laser power and **e,** cortical depth, where % inactivation is relative to cell's spike rate during laser-off trials. **f,** Lateral extent of inactivation. Illumination of 20–40 mW reliably inactivated an area within a 1-mm radius. **g,** Photoinhibition at 40 mW fully blocked spontaneous and sensory-evoked spikes (100% inactivation relative to laser-off trials) in 83% of RS cells and >96% of spikes in 94% of RS cells (same cells as in panel c). **h,** Fast-spiking (FS) neurons (n = 8 cells) were similarly silenced. **i,** Estimated area of photoinhibition with 40-mW relative to barrel cortex (1-mm radius around C2 barrel, red circle) depicted with a tangential section through barrel cortex of an Nr5a1-eYFP mouse with layer 4 labeled to visualize barrels. **j,** Emx1-Halo-mediated cortical inactivation was also assessed during detection behavior with array recordings (n=8 session, 3 mice). **k,** Same data from Fig. 1e replotted on a logarithmic scale to show low spike rates during laser on trials. **l,** Behavioral performance during laser off and on trials did not correlate with spiking activity for each trial type (4 sessions from 3 mice with % correct for laser-off trials: 82, 87, 80, and 78%). **m,** Laser-on data in **l,** replotted with larger scale to visualize data during laser-on trials. Error bars: **d-h**, median ± interquartile range. **l,m**, mean and S.E.M.

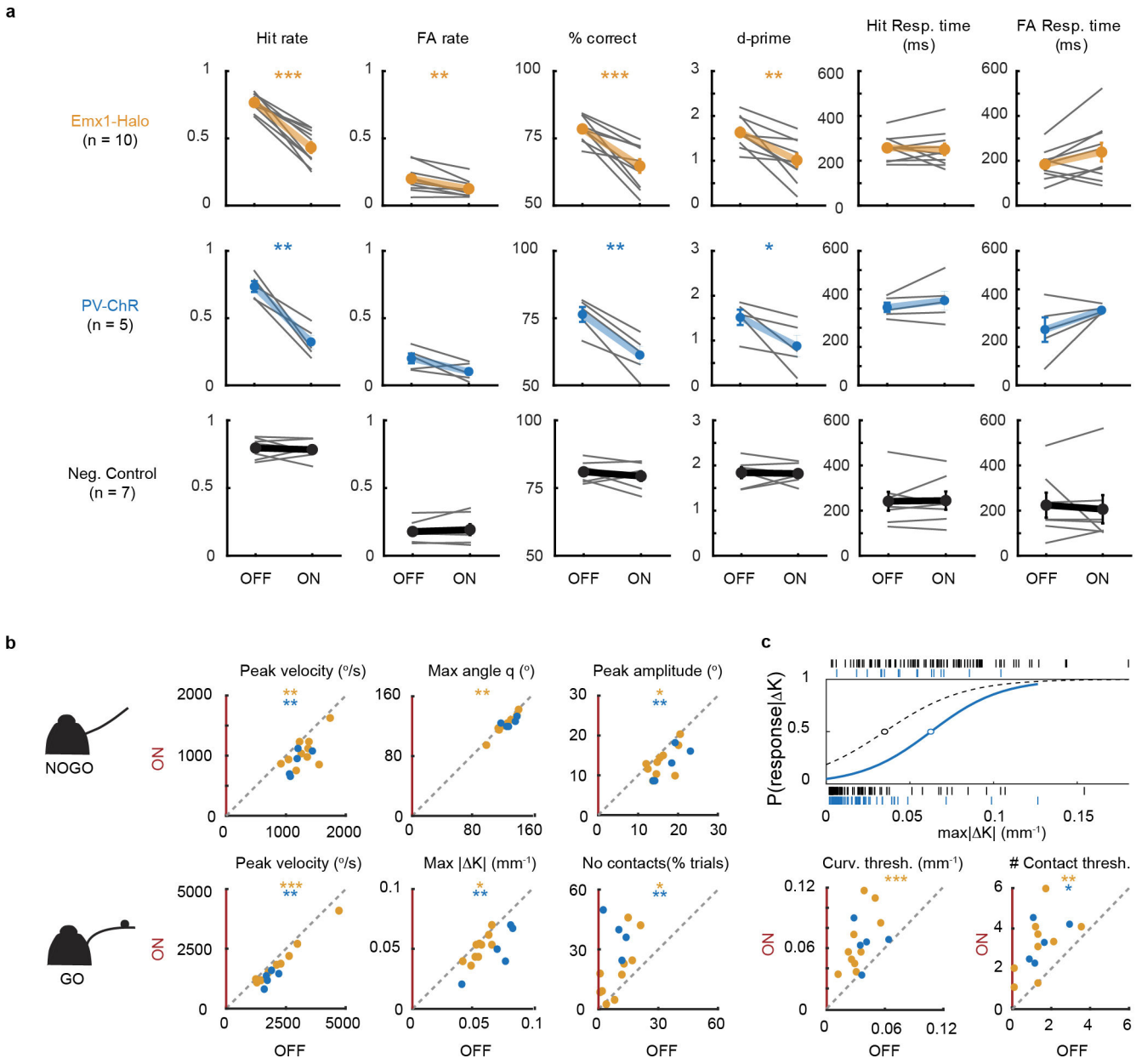

Extended Data Figure 2 |. Optogenetic manipulations of barrel cortex using PV-ChR and Emx1-Halo result in similar behavioral, motor, and sensory deficits.

a, Photoinhibition of excitatory neurons in Emx1-Halo (orange) and photoactivation of inhibitory neurons in PV-ChR (blue) yielded similar behavioral deficits. Negative control animals (Cre-negative, stop-Halo mice, black) were unaffected by 593-nm laser illumination. **b,** Both Emx1-Halo and PV-ChR photostimulation decrease whisking kinematics and **c**, increase sensory thresholds. Data for negative control and Emx1-Halo are the same as in Figures 2 and 3 but repeated here for comparison with PV-ChR.

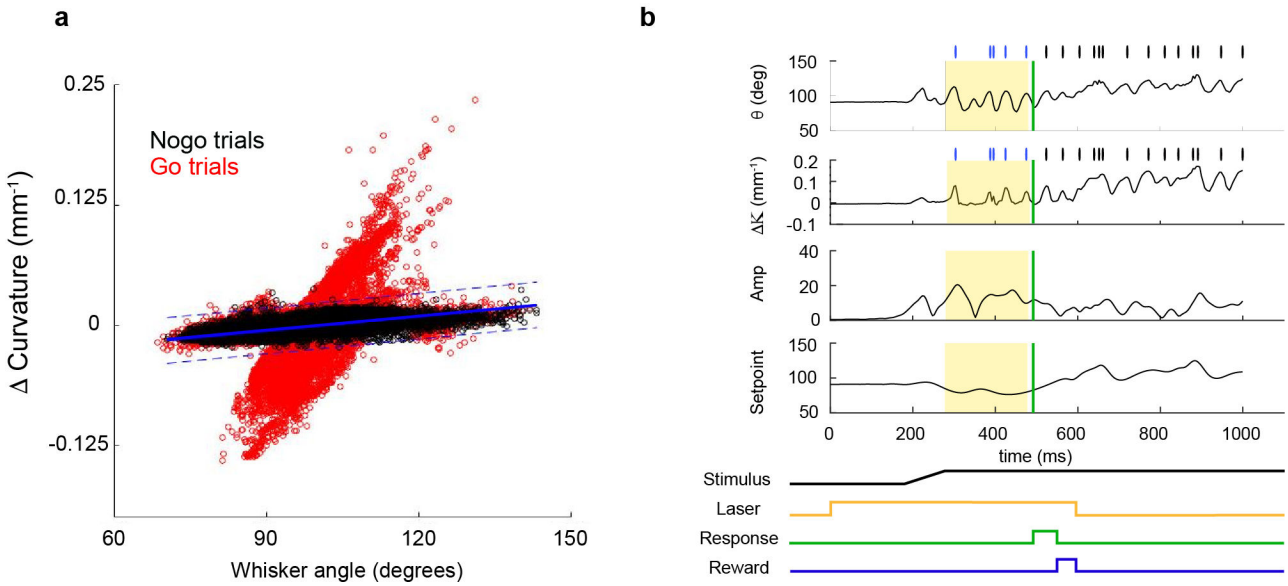

Extended Data Figure 3 |. Defining contacts based on whisker angle and change in curvature. **a,** Example curvature versus whisker position for a single session. Each circle represents the paired values for curvature and whisker angle for each frame during the session. Values for nogo trials define whisker parameters during free whisking in air, when no contacts can be made (black); and go trials are shown in red. Linear regression was used to define the line of best fit (blue, solid line) for nogo parameters, and upper and lower contact thresholds were set by finding the offsets that encompassed the no-contact parameter space (1–5 standard deviations from the line-of-best-fit, blue dotted lines). **b,** Putative contacts were defined as points at which the local maxima or minima of the change in curvature were above (forward contact with whisker) or below (reverse contact with whisker) the defined thresholds (tick marks). Whisking analysis was restricted to the 200-ms time window (yellow shaded area) during sampling, before the response (green).

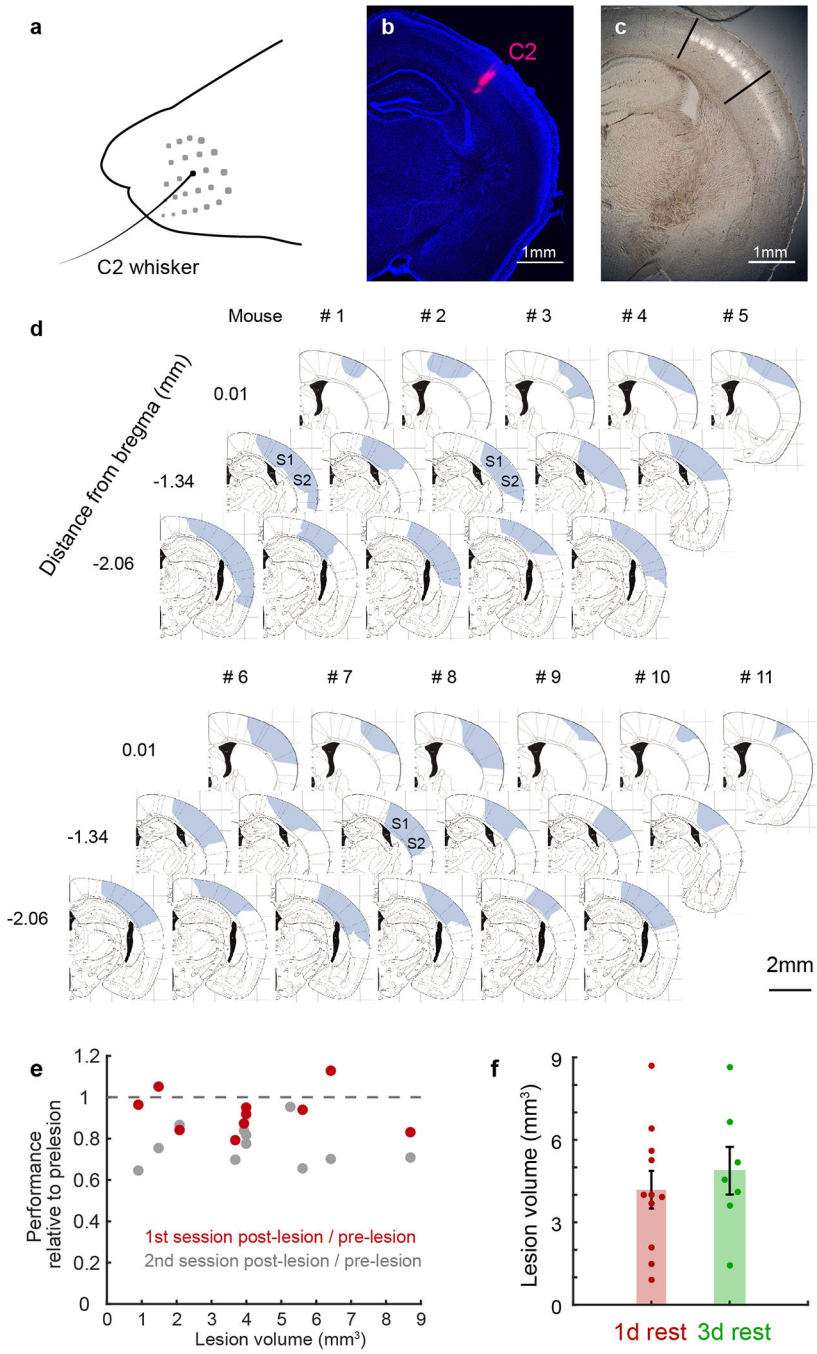

Extended Data Figure 4 |. Behavioral performance after lesions did not correlate with lesion size.

a, Mice performed the task with a single C2 whisker. **b,** The location of the C2 barrel in a coronal section. The C2 barrel was functionally mapped with intrinsic imaging and Alexa-conjugated cholera toxin subunit B (CTB, red) was injected into the center of the C2 barrel. Blue: DAPI. Mappings in b and c are used to inform the location of lesions made relative to the C2 barrel column. **c,** Equivalent location in section of an Nr5a1-eYFP animal with barrels fluorescently labeled in L4 (white) overlaid on bright-field image to show extent of barrel cortex relative to section (black lines). C2 was located ~1.2–1.5 mm posterior to

bregma, varying slightly between animals. Lesions were centered around C2. **d,** Size and locations of contralateral barrel cortex lesions for the 11 mice with 1-day rest shown in Fig. 3 (arranged from largest to smallest by lesion volume). For each mouse, three locations along the anterior-posterior axis are shown overlaid on atlas images reproduced with permission from Paxinos & Franklin, 2001[42]. In a few mice (e.g., mouse 1, 3, 8), lesions extended into the secondary somatosensory area (S2). Numbers along anteroposterior axis indicate approximate location relative to bregma. **e,** Lesion size did not correlate with the degree of impairment on the first (gray) or second post-lesion session when behavioral performance recovers (red). Performance was normalized to the pre-lesion performance for each animal. **f,** Lesion sizes were similar between groups with 1 or 3-days of rest after lesioning.

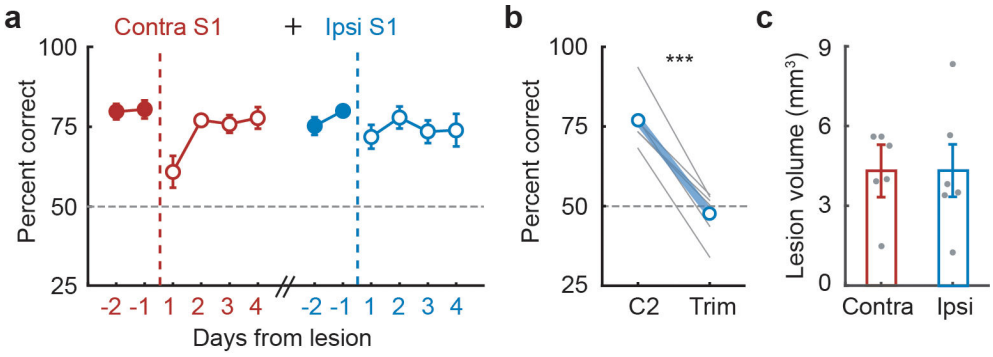

Extended Data Figure 5. Ipsilateral S1 does not compensate for loss of contralateral S1.

a, Behavioral performance of mice rapidly recovered after contralateral S1 lesions as shown in Fig.3c (red). Subsequent ipsilateral lesion (n=6) was similar to sham and ipsi-only manipulations shown in Fig.3c, indicating that ipsilateral S1 was not compensating for loss of contralateral S1 activity. **b,** C2 whisker trim control. Performance of bilaterally lesioned animals dropped to chance when the C2 whisker was removed. **c,** Size of bilateral lesions.

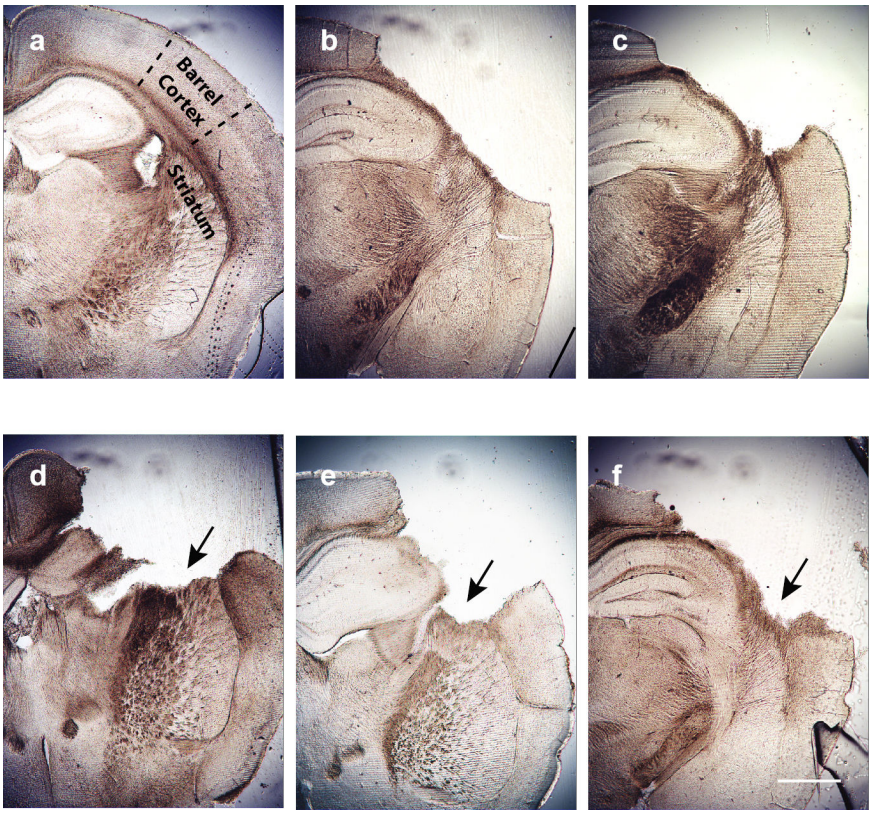

Extended Data Figure 6 |. Example histology from lesioned animals depicting contralateral S1 only or additional damage to striatum.

a, Unlesioned example, **b-c,** examples of S1-only lesions from 2 mice. **d-f,** 3 examples of damage to striatum in addition to S1. Even minimal damage (arrows) to the dorsolateral striatum resulted in permanent behavior deficits. Scalebar: 1 mm

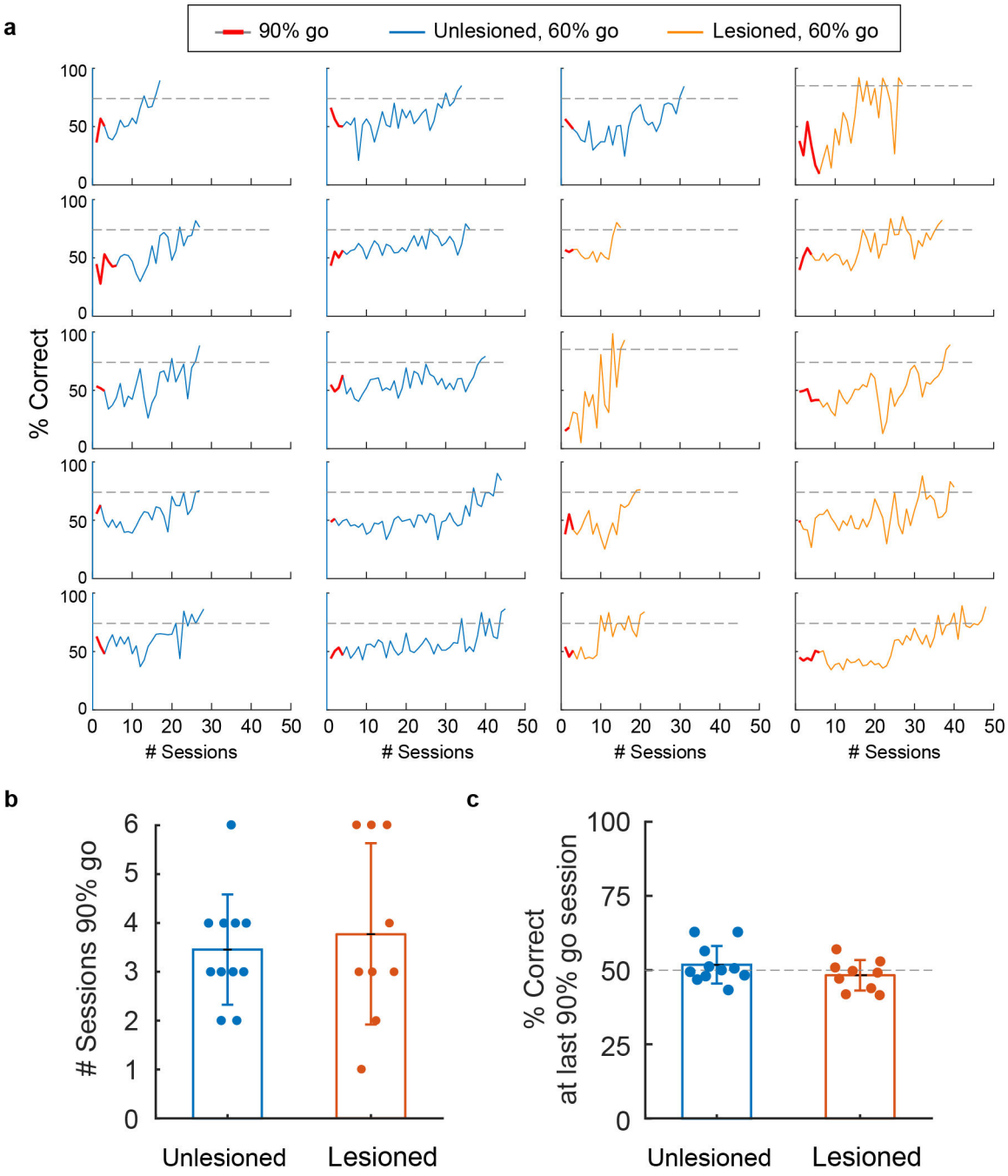

Extended Data Figure 7 |. Learning curves for unlesioned and lesioned mice in learning experiment.

a, Individual learning curves for unlesioned (n=11, blue lines) and contralateral barrel cortex lesioned mice (n=9, orange lines) that learned the detection task to criterion (74% correct performance for 2 consecutive sessions). Animals were first introduced to the pole with 90% go trials (red lines). This intermediate step ensured that animals maintained a stable weight before moving on to the last step of training. Mice were moved onto 60% go trials for the rest of the learning assessment. Animals were given 48 sessions to learn the task, **b,** Unlesioned and lesioned groups spent similar time on 90% go sessions (3.8±1.8 vs. 3.5±1.1

sessions for unlesioned and lesioned mice, respectively, p = 0.63). **c,** By the end of the 90% go sessions, animal performance was still at chance levels (p=0.34, p = 0.37 for unlesioned and lesioned mice, respectively, one-sample t-test).

Supplementary Material

Refer to Web version on PubMed Central for supplementary material.

Acknowledgements

We thank B. Christina Pil and Ayano Kase for assistance with animal training, Hongkui Zeng for suggesting Ai39 mice, Attila Losonczy for PV-Cre mice, Josh Huang for Rosa-H2B-GFP mice, Nathan Clack for suggestions on video analysis of whisker motion, and Benjamin Grewe for advice on cortical aspiration. We also thank Juan Carlos Tapia, Mickey Goldberg, Nate Sawtell, Tom Jessell, Amanda Kinnischtzke, Dan Kato, and Georgia Pierce for comments on the manuscript. Funding was provided by NIH R01 NS094659, R01 NS069679, the Klingenstein Fund, the Rita Allen Foundation, the Dana Foundation, and the Ludwig Schaefer Scholars Program (RMB); NIH F32 NS055488 (YKH), T32 MH015174 (YKH, COL), and F32 NS096819 (CCR).

References

1. Glickfeld LL, Histed MH & Maunsell JHR Mouse primay visual cortex is used to detect both orientation and contrast changes. J. Neurosci 33, 19416–22 (2013). [PubMed: 24336708]
2. Petruno SK, Clark RE & Reinagel P Evidence That Primary Visual Cortex Is Required for Image, Orientation, and Motion Discrimination by Rats. PLoS One 8, 1–10 (2013).
3. Lashley KS The mechanism of vision IV. The cerebral areas necessary for pattern vision in the rat. J. Comp. Neurol 53, 419–478 (1931).
4. Kato HK, Gillet SN & Isaacson JS Flexible Sensory Representations in Auditory Cortex Driven by Behavioral Relevance. Neuron 88, 1027–1039 (2015). [PubMed: 26586181]
5. Kelly JB & Glazier SJ Auditory cortex lesions and discrimination of spatial location by the rat. Brain Res 145, 315–321 (1978). [PubMed: 638790]
6. Talwar SK, Musial PG & Gerstein GL Role of mammalian auditory cortex in the perception of elementary sound properties. J. Neurophysiol 85, 2350–2358 (2001). [PubMed: 11387381]
7. Oliveira-Maia AJ et al. The Insular Cortex Controls Food Preferences Independently of Taste Receptor Signaling. Front. Syst. Neurosci 6, 1–13 (2012). [PubMed: 22291622]
8. Peng Y et al. Sweet and bitter taste in the brain of awake behaving animals. Nature 527, 512–515 (2015). [PubMed: 26580015]
9. Waiblinger C, Brugger D & Schwarz C Vibrotactile discrimination in the rat whisker system is based on neuronal coding of instantaneous kinematic cues. Cereb. Cortex 25, 1093–1106 (2015). [PubMed: 24169940]
10. Hutson KA & Masterton RB The sensory contribution of a single vibrissa's cortical barrel. J. Neurophysiol. 56, 1196–1223 (1986). [PubMed: 3783236]
11. Morita T, Kang H, Wolfe J, Jadhav SP & Feldman DE Psychometric curve and behavioral strategies for whisker-based texture discrimination in rats. PLoS One 6, e20437 (2011). [PubMed: 21673811]
12. Guo ZV et al. Flow of cortical activity underlying a tactile decision in mice. Neuron 81, 179–194 (2014). [PubMed: 24361077]
13. O'Connor DH, Peron SP, Huber D & Svoboda K Neural activity in barrel cortex underlying vibrissa-based object localization in mice. Neuron 67, 1048–1061 (2010). [PubMed: 20869600]
14. Kwon SE, Yang H, Minamisawa G & O'Connor DH Sensory and decision-related activity propagate in a cortical feedback loop during touch perception. Nat. Neurosci 19, 1243–1249 (2016). [PubMed: 27437910]
15. Miyashita T & Feldman DE Behavioral detection of passive whisker stimuli requires somatosensory cortex. Cereb. Cortex 23, 1655–62 (2013). [PubMed: 22661403]

16. Sachidhanandam S, Sreenivasan V, Kyriakatos A, Kremer Y & Petersen CCH Membrane potential correlates of sensory perception in mouse barrel cortex. Nat. Neurosci. 16, 1671–7 (2013). [PubMed: 24097038]
17. Stüttgen MC & Schwarz C Barrel cortex: What is it good for? Neuroscience (2017). doi:10.1016/j.neuroscience.2017.05.009
18. Otchy TM et al. Acute off-target effects of neural circuit manipulations. Nature 528, 358–363 (2015). [PubMed: 26649821]
19. Deutsch D, Pietr M, Knutsen PM, Ahissar E & Schneidman E Fast Feedback in Active Sensing: Touch-Induced Changes to Whisker-Object Interaction. PLoS One 7, (2012).
20. Grant RA, Mitchinson B, Fox CW & Prescott TJ Active touch sensing in the rat: anticipatory and regulatory control of whisker movements during surface exploration. J Neurophysiol 101, 862–874 (2009). [PubMed: 19036871]
21. Mitchinson B et al. Active vibrissal sensing in rodents and marsupials. Philos. Trans. R. Soc. Lond. B. Biol. Sci 366, 3037–48 (2011). [PubMed: 21969685]
22. Matyas F et al. Motor Control by Sensory Cortex. Science 330, 1240–1244 (2010). [PubMed: 21109671]
23. Harvey M Sachdev a,, Zeigler RN, H. P. Cortical barrel field ablation and unconditioned whisking kinematics. Somatosens. Mot. Res 18, 223–227 (2001). [PubMed: 11562085]
24. Pammer L et al. The Mechanical Variables Underlying Object Localization along the Axis of the Whisker. J Neurosci 33, 6726–6741 (2013). [PubMed: 23595731]
25. Stüttgen MC & Schwarz C Psychophysical and neurometric detection performance under stimulus uncertainty. Nat. Neurosci 11, 1091–1099 (2008). [PubMed: 19160508]
26. Keck T et al. Synaptic scaling and homeostatic plasticity in the mouse visual cortex in vivo. Neuron 80, 327–334 (2013). [PubMed: 24139037]
27. Kawai R et al. Motor Cortex Is Required for Learning but Not for Executing a Motor Skill. Neuron 86, 800–812 (2015). [PubMed: 25892304]
28. Brecht M Perspective The Body Model Theory of Somatosensory Cortex. Neuron 94, 985–992 (2017). [PubMed: 28595055]
29. Stüttgen MC, Schwarz C & Jäkel F Mapping spikes to sensations. Front. Neurosci 5, 1–17 (2011). [PubMed: 21390287]
30. Cohen JD & Castro-alamancos MA Detection of Low Salience Whisker Stimuli Requires Synergy of Tectal and Thalamic Sensory Relays. J. Neurosci 30, 2245–2256 (2010). [PubMed: 20147551]
31. Huerta MF, Frankfurter A & Harting JK Studies of the principal sensory and spinal trigeminal nuclei of the rat: Projections to the superior colliculus, inferior olive, and cerebellum. J. Comp. Neurol 220, 147–167 (1983). [PubMed: 6643723]
32. Smith JB, Mowery TM & Alloway KD Thalamic POm projections to the dorsolateral striatum of rats: potential pathway for mediating stimulus-response associations for sensorimotor habits. J. Neurophysiol. 108, 160–174 (2012). [PubMed: 22496533]
33. Gorski J et al. Cortical excitatory neurons and glia, but not GABAergic neurons, are produced in the Emx1-expressing lineage. J. Neurosci 22, 6309–14 (2002). [PubMed: 12151506]
34. Scholl B, Pattadkal JJ, Dilly GA, Priebe NJ & Zemelman BV Local Integration Accounts for Weak Selectivity of Mouse Neocortical Parvalbumin Interneurons. Neuron 87, 424–437 (2015). [PubMed: 26182423]
35. O'Connor DH et al. Vibrissa-based object localization in head-fixed mice. J. Neurosci 30, 1947–1967 (2010). [PubMed: 20130203]
36. Clack NG et al. Automated Tracking of Whiskers in Videos of Head Fixed Rodents. Plos Comput. Biol 8, e1002591 (2012). [PubMed: 22792058]
37. Hill DN, Curtis JC, Moore JD & Kleinfeld D Primary motor cortex reports efferent control of vibrissa motion on multiple timescales. Neuron 72, 344–356 (2011). [PubMed: 22017992]
38. Kleinfeld D & Deschênes M Neuronal basis for object location in the vibrissa scanning sensorimotor system. Neuron 72, 455–68 (2011). [PubMed: 22078505]
39. Bruno RM & Simons DJ Feedforward Mechanisms of Excitatory and Inhibitory Cortical Receptive Fields. J. Neurosci 22, 10966–10975 (2002). [PubMed: 12486192]

40. Pachitariu M, Steinmetz N, Kadir S, Carandini M & Harris KD Kilosort: realtime spike-sorting for extracellular electrophysiology with hundreds of channels. bioRxiv (2016). doi:10.1101/061481

41. Rossant C et al. Spike sorting for large, dense electrode arrays. Nat. Neurosci 19, 634–641 (2016). [PubMed: 26974951]

42. Paxinos G & Franklin KB J. *The mouse brain in stereotaxic coordinates*. 2nd ed, (Academic Press, 2001).

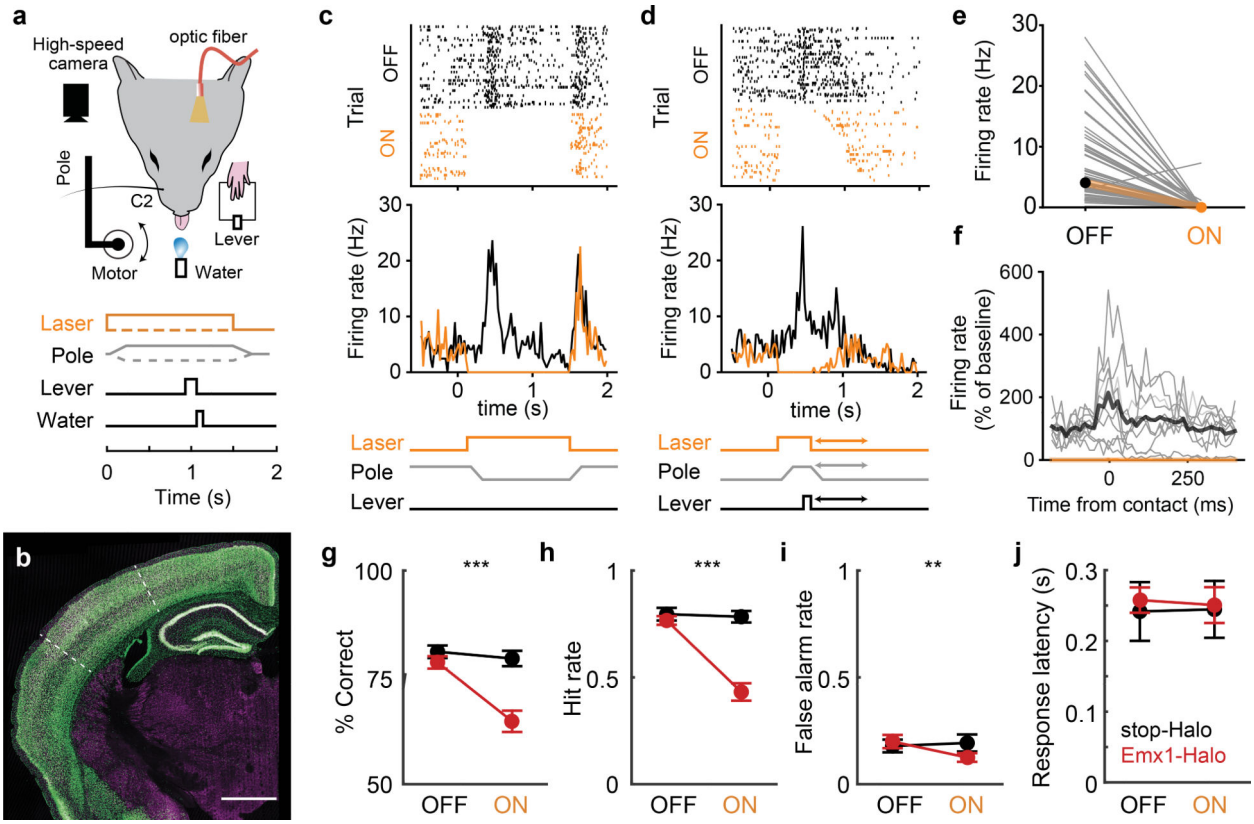

Figure 1 |. Transient inactivation of barrel cortex impairs whisker-mediated detection.

a, Head-fixed detection ask. A high-speed camera imaged whiskers. Pole movement (go/nogo) and laser (on/off) were randomized across trials. **b,** Coronal section of Emx1-GFP mouse. White dotted line: barrel cortex boundaries; green: GFP; magenta: NeuN. **c,** Cortical array recordings during detection task and photoinactivation. Example rasters (top) and PSTHs (middle) for a single unit when no response was made (miss/correct reject) during an example session. **d,** Same neuron for trials with lever response (hit/false alarm). The laser turns off when animal responds, ending the trial. Trials sorted by response time, which varied (arrows in schematic at bottom). **e,** Effect of laser on neuronal spiking (n=62 putative excitatory neurons, 8 sessions, 3 mice; mean±SD 7.02±6.81and 0.16±0.94 Hz for laser off vs on, respectively). **f,** Average spiking activity aligned to first whisker contact of trial during an example session (n=10 neurons). Contact times are defined as the local maxima, rather than onset, of curvature change (see Extended Data Fig. 3 and Methods). Firing rates were normalized to mean rate during 100 ms prior to contact during laser-off trials. Thin lines: individual cells, thick lines: means. Behavioral performance for laser off vs on trials: **g,** % correct trials **h,** Hit rate; **i,** False alarm rate. **j,** Response latency for hit trials. Emx1-Halo (n = 10 mice, red), negative control (n = 7 cre-negative, stop-Halo mice, black). Error bars: means ± SEMs. Scale bar: 1mm.

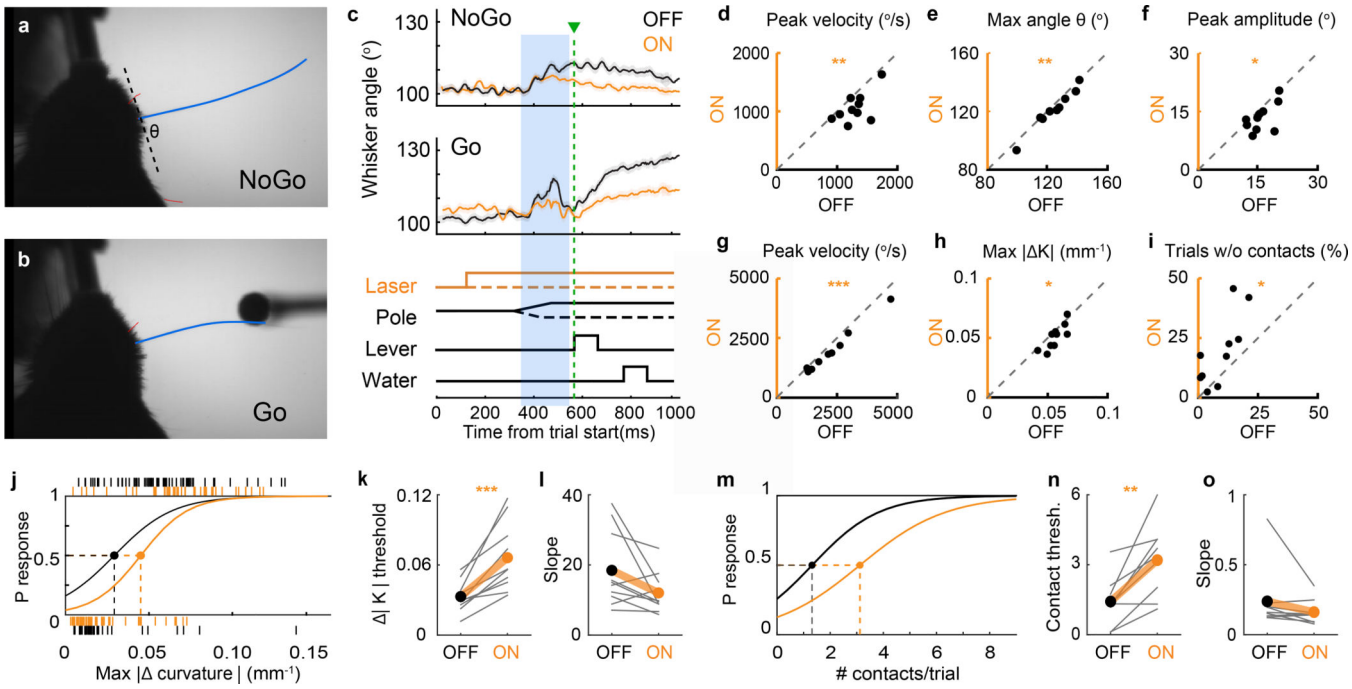

Figure 2 |. Transient optogenetic inactivation of barrel cortex alters whisking kinematics and sensory threshold.

a, High-speed video frame depicting traced C2 whisker during nogo trial (pole moves away); and **b,** go-trial (pole within whisker reach). Whisker position was measured as its angle (θ) relative to the face. The whisker bends upon contacting pole, changing whisker curvature. **c,** Average whisker angle for nogo and go trials for an example session. A 200-ms window (blue shaded area), from when the pole was within reach and before the response, was analyzed. Green: average response time. Whisking kinematics for each animal during nogo trials: **d,** peak angular velocity of whisker protraction; **e,** maximum whisker angle; and **f,** mean peak whisking amplitude. For go trials: **g,** peak angular protraction velocity, **h,** average maximum change in curvature (ΔK), and **i,** % of trials without any contacts. **j,** Logistic regression of response probability given max Δcurvature for an example session. Tick marks indicate responses (0 for no response; 1 for lever response) on individual trials. Detection threshold was defined as the value at which response probability is 0.5. **k,** Detection threshold for maximum ΔK, and **l,** slope (sensitivity) for each animal. **m,** Logistic regression of response probability against number of contacts/trial for an example session. **n,** Detection threshold for number of contacts and **o**, slope.

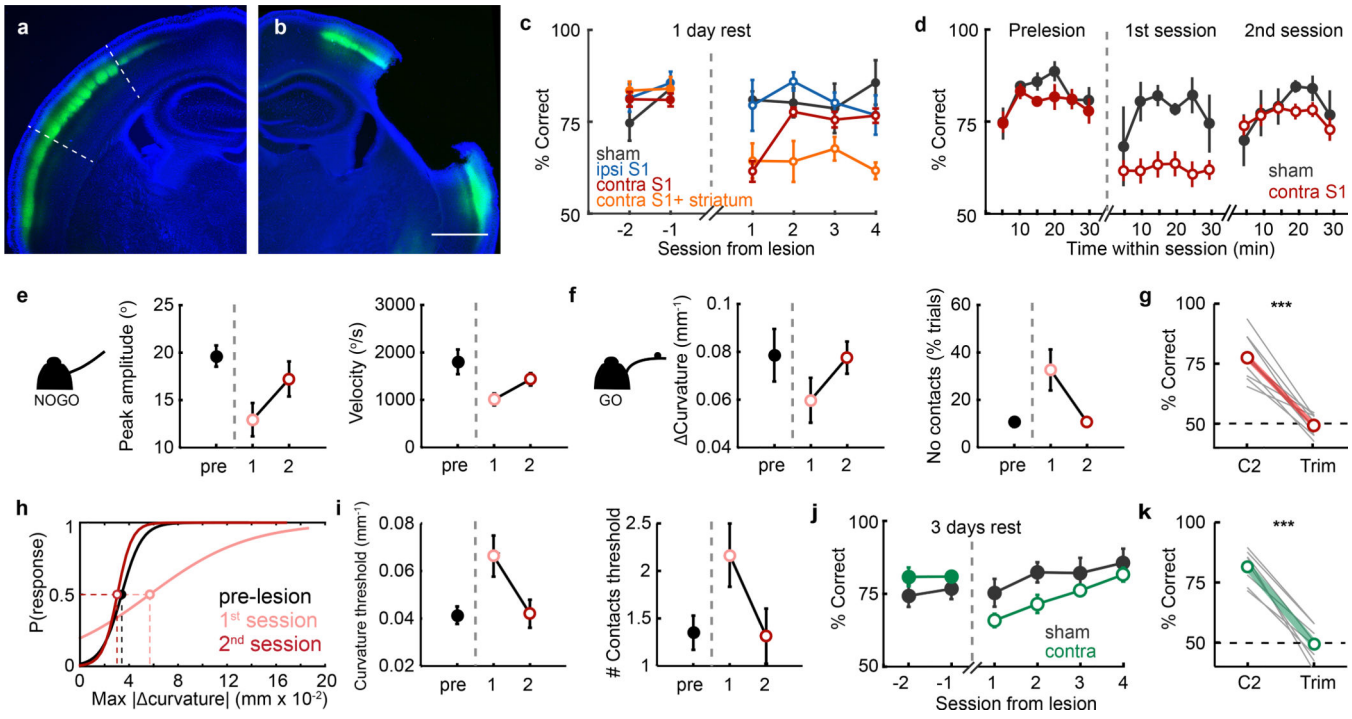

Figure 3 |. Behavioral performance rapidly recovers after barrel cortex lesions.

a, Coronal section of L4-labeled mouse (white dashed line: barrel cortex boundaries; blue, DAPI; green, eYFP) in unlesioned hemisphere. **b,** Lesioned hemisphere shows complete removal of barrel cortex. **c,** Behavioral performance before and after S1 lesions (sham n=5, ipsilateral n=4, contralateral n=11, contralateral with striatal lesion n=8). **d,** Behavioral performance of contralateral S1 lesioned animals recovers abruptly between first and second post-lesion sessions. **e,** Whisking kinematics during nogo trials and **f,** go trials of mice are altered on 1st post-lesion session but return to normal by 2nd post-lesion session (n=10 contra mice). **g,** Post-lesion trimming confirms task remained whisker-dependent. Dashed line indicates chance performance. **h,** Example logistic regression of response probability given whisker curvature. Sensory detection threshold for whisker curvature increases on 1st session post-lesion (pink), returning to pre-lesion levels (black) by second session (red). **i,** Average detection thresholds for whisker curvature and number of contacts pre- and 2 sessions post-lesion (n = 10). **j,** Animals with 3 days of rest after lesion still had impaired performance on the 1st post-lesion session but subsequently recovered (n=8). **k,** Behavioral performance for 3-day rest group remains whisker dependent.

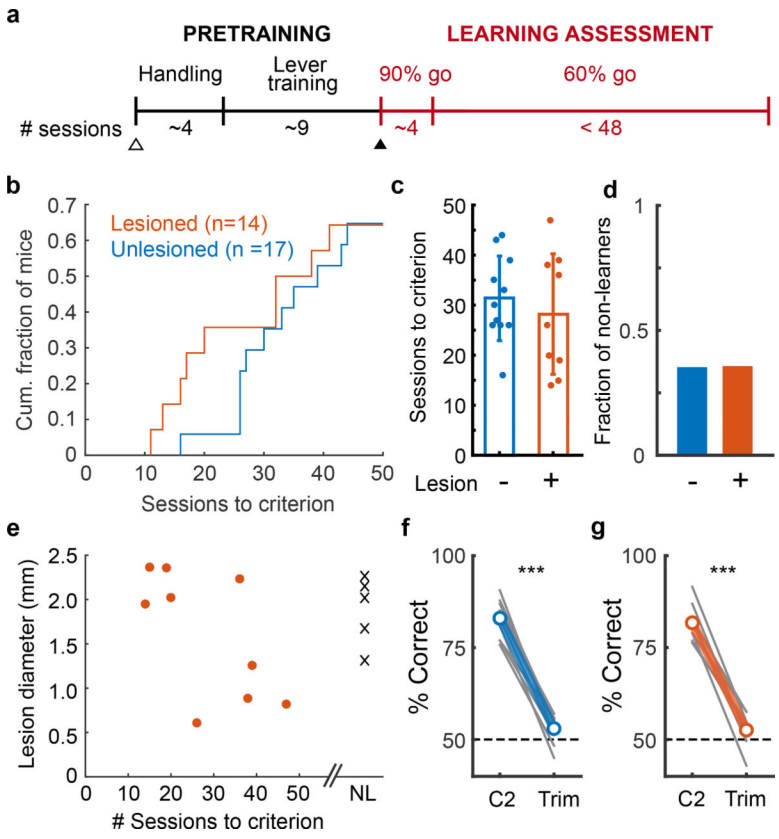

Figure 4 |. Barrel cortex is not required for learning whisker-dependent sensory detection task.

a, Timeline for learning assay. **b,** Cumulative histogram of number of sessions to reach learning criterion (74% correct for 2 consecutive sessions). The speed of learning was similar between unlesioned (n=17) and lesioned (n=14) mice. **c,** Among mice that learned the task, the number of sessions to criteria did not differ between unlesioned (n=11) and lesioned (n=9) animals. **d,** The fraction of mice that did not learn within the assessment period (45 sessions) was similar between groups (unlesioned n=6, lesioned n=5 mice). **e,** Inability to learn was not due to larger lesion size, NL, non-learners. **f,** Unlesioned and **g,** lesioned mice that did learn could no longer perform the task when the C2 whisker was trimmed.